ISBN: 978-3-95450-205-9   doi:10.18429/JACoW-Cyclotrons2019-MOP025

FAST RECHARGING OF ELECTROSTATIC INJECTION AND EXTRACTION SEPTA AFTER BREAKDOWN

R. Dölling†, Paul Scherrer Institut, 5232 Villigen PSI, Switzerland
J. Brutscher, 01324 Dresden, Germany

Abstract

We propose to recharge an electrostatic injection or extraction septum in a high-power cyclotron fast enough to omit the need for switching off the beam at a high voltage breakdown.

INTRODUCTION

In the Ring cyclotron, a proton beam of up to 2.4 mA is injected and extracted with the help of electrostatic septa [1]. Depending on tuning status, conditioning, actual problems and actual beam current, 5 to 300 short beam trips occur per day, from which ~1/10 include high voltage (HV) breakdowns in these septa. However, we do not know whether the breakdown is the reason or a consequence of beam switch off and related interlocks of loss monitors indicating errant beam. Anyhow, then the beam is switched off and ramped up again in about half a minute. This already amounts to a large fraction of the unscheduled downtime of the accelerator [2]. Some 5% of the experiments at the subsequent spallation source SINQ, as 2D or 3D imaging of processes, suffer from information loss due to these interruptions [3]. Also, the frequent beam switch-off and corresponding thermal cycling may accelerate the ageing of the SINQ target [4]. As a remedy for that fraction of beam trips, which are caused by a septum, we propose a recharging of the septum within 1 ms, which would allow to keep the beam running, being lost only for this short time. The amount of uncontrolled beam loss and the needed reaction times for surveillance is comparable to the switching of the full beam between beam lines routinely performed for the operation of the ultra-cold neutron source UCN [5]. Furthermore, for interlocks caused by other transients, detected, e.g., by loss monitors, a fast recharge of the septa may also allow to keep the beam running, if the causes decay correspondingly fast. The required fast surveillance will be eased by the new generation of loss monitor read-out electronic under preparation [6].

ACTUAL SETUP

The electrical (Fig. 1) and mechanical (Fig. 2) setup is discussed in the context of the injection septum EIC. The HV supply located outside the vault is connected to the septum via a long HV cable, a CERN type [7] external isolation resistor, a vacuum feedthrough, an in-vacuum damping resistor and a flexible connection to the cathode, which allows the mechanical adjustment of the septum during operation. A breakdown nearly fully discharges septum and short cable to isolation resistor, but not the long cable, since the discharge cannot be maintained with a low current. The exchange of charge already stored in the long cable and the power supply takes ~8 ms and recharges the cathode already to ~93% of the nominal 134 kV. Then the power supply delivers a charging current, typically limited to 100 µA, for ~0.6 s. With most breakdowns, a standard load curve is precisely reproduced (Fig. 3). During loading, the beam is already switched off due to beam losses or the low-voltage indication of the HV supply. Occasionally, multiple breakdowns occur (Fig. 4), or deeper breakdowns, which are also likely to be "assembled" by consecutive, but not resolved sparks. We also see switch off due to low-voltage indication resulting from overly increased dark current induced by operation of the nearby radial probe RRL [8].

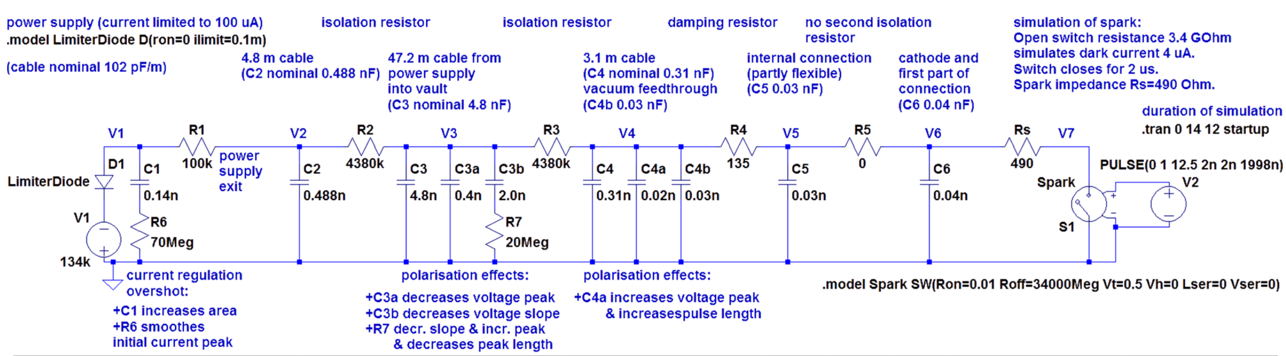

HV supply cur limit	R3	R4	R5	Rs		V2max	V3max	V4max	I1max	I2max	I3max	I4max	I5max	Ismax	V6 deficit after 1 ms	V6 deficit <1 kV after	HV supply in cur limit for
100 uA	4.38 MΩ	135 Ω	0 Ω	490 Ω	actual operation	-126.2 kV	-125.2 kV	~0 kV	168 uA	937 uA	31 mA	178 A	-	266 A	82 kV	511 ms	559 ms
500 uA	4.38 MΩ	135 Ω	0 Ω	490 Ω	increased current limit	-128.3 kV	-125.5 kV	~0 kV	553 uA	1.16 mA	31 mA	173 A	-	266 A	82 kV	107 ms	79 ms
500 uA	350 kΩ	135 Ω	0 Ω	490 Ω	lower Risol	-127.9 kV	-124.0 kV	~0 kV	561 uA	2.0 mA	382 mA	173 A	-	266 A	10.2 kV	105 ms	80 ms
500 uA	350 kΩ	1 MΩ	0 Ω	1200 Ω	plus 2nd Risol (instead Rdamp)	-134.0 kV	-132.3 kV	-122.3 kV	370 uA	370 uA	32 mA	134mA	-	111 A	1.8 kV	13 ms	-
500 uA	350 kΩ	135 Ω	1 MΩ	1600 Ω	plus 2nd Risol (new)	-134.0 kV	-133.0 kV	-125.8 kV	217 uA	217 uA	23 mA	123 mA	134 mA	83 A	1.05 kV	1.1 ms	-
100 uA	350 kΩ	135 Ω	1 MΩ	1600 Ω	plus 2nd Risol (new)	-133.6 kV	-133.0 kV	-125.8 kV	109 uA	201 uA	23 mA	123 mA	134 mA	83 A	1.05 kV	1.1 ms	29 ms

Figure 1: Present electrical circuit. Rs chosen to approximate calculated curves in Fig. 5 by V6. Its value corresponds to arc resistance at passing 75 kV. C4b, C5, C6 estimated from geometry. Simulation results are given for variants as well.

† rudolf.doelling@psi.ch

ISBN: 978-3-95450-205-9 doi:10.18429/JACoW-Cyclotrons2019-MOP025

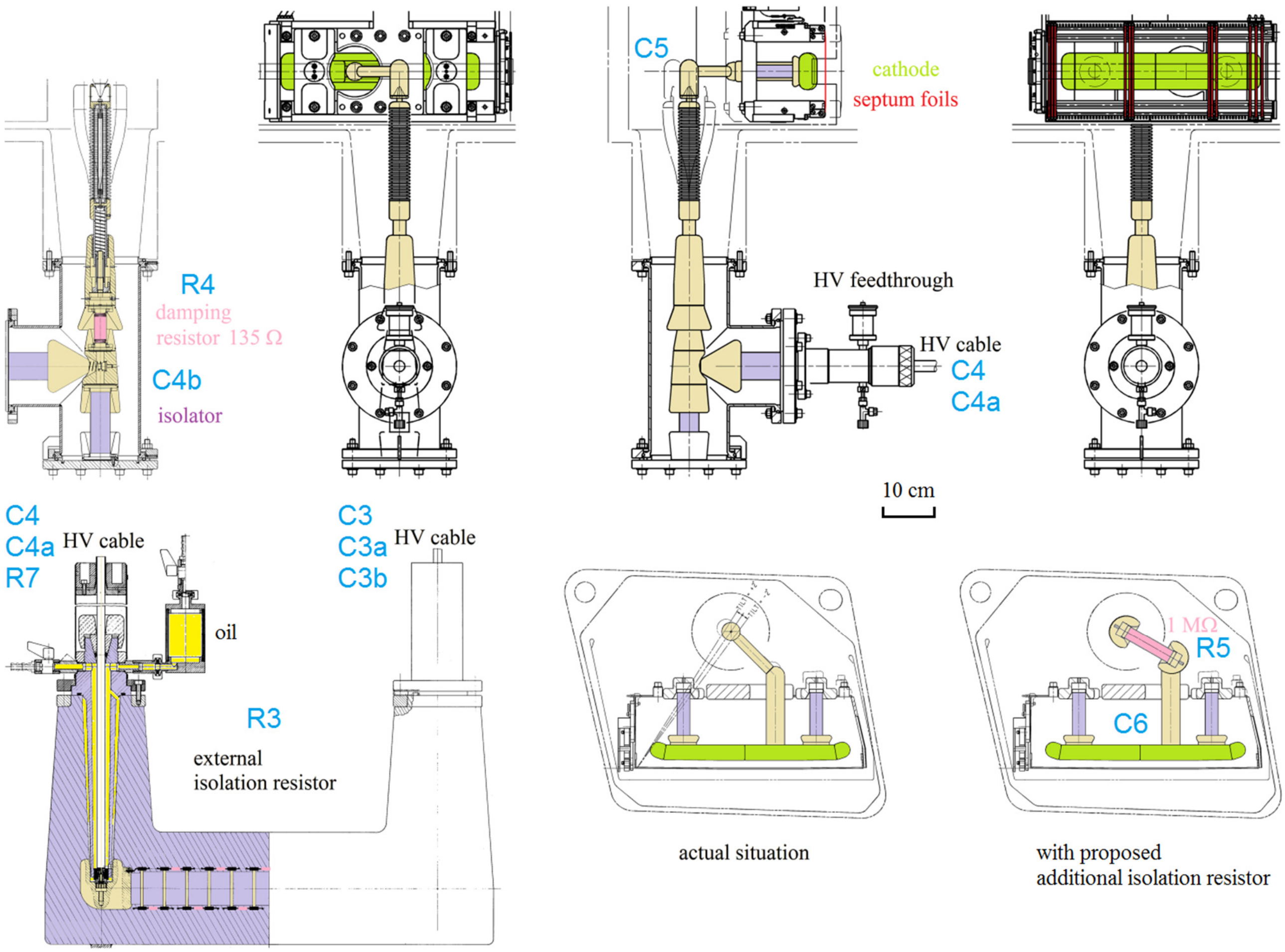

Figure 2: Mechanical setup of injection septum EIC of the Ring cyclotron. Shielded HV cables of type 2134 [9].

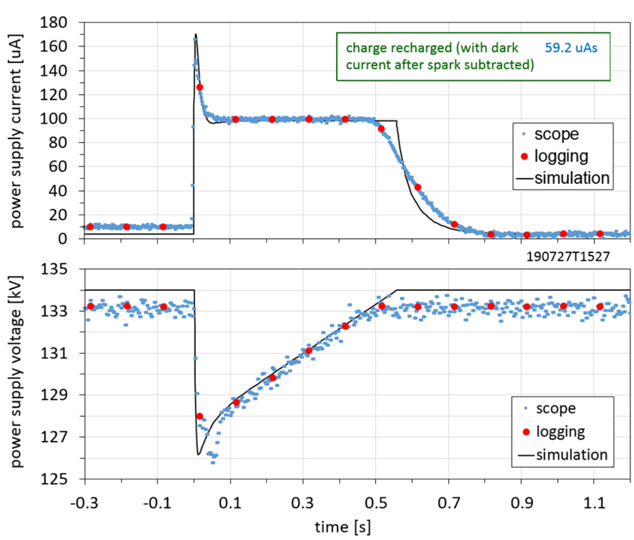

Figure 3: HV supply load curves for a “standard” spark. Current and voltage readings from HV supply analogue outputs at a scope. In addition, the data logged by the control system and the results from the LTspice simulation from Fig. 1 are depicted.

The initial current peak is probably caused by a non-ideal current regulation. In the LTspice simulation [10], this is roughly reproduced by adding C1, R6. The initial voltage peak, as well as the final slow current drop, result from polarisation currents in the dielectrics of the isolators. This is represented in the simulation by C3a, C3b, R7, C4a. However, the final current drop could not be reproduced exactly. Also, the result is still reasonable with R7 much lower, even 0 Ohm. In any case, cable capacitance is significantly increased above the specified value.

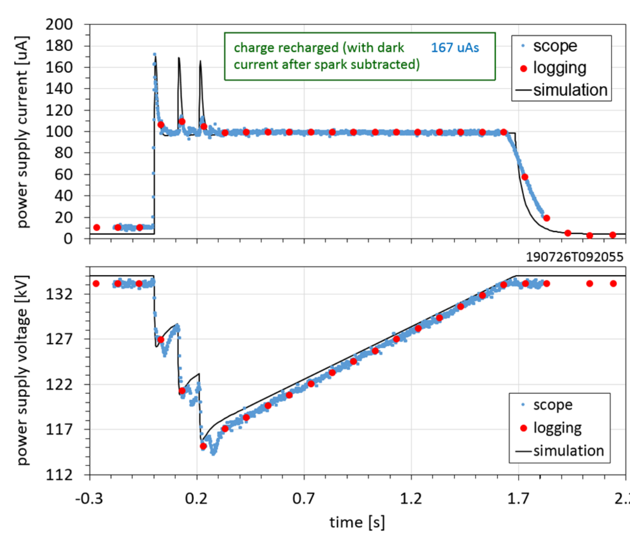

Figure 4: Triple breakdown.

ISBN: 978-3-95450-205-9 doi:10.18429/JACoW-Cyclotrons2019-MOP025

For the long cable, this, e.g., corresponds to an increase of the diameter of the inner conductor from 5.6 mm (4.8 nF) to 8.5 mm (7.2 nF), thereby decreasing the isolation distance from 6.9 mm to 5.4 mm. Possibly, this is an indication of degradation of the cable isolator. It will be interesting to see if this could help to identify critically aged cables.

PROPOSED SETUP

In an improved setup, the external isolation resistor close to the vacuum chamber would be smaller, e.g., 350 kΩ, as used for the CERN PSR septa [11], leading to a much faster initial redistribution of charge. 124 kV would be reached after the critical loss duration of 1 ms. Tests with deactivated beam centring demonstrated, that a static beam of 1730 µA or less is transported within a window of cathode voltage of ~120 kV to 140 kV. With a delayed switch-off, the shortly interrupted beam should be transported as well.

However, at higher beam currents, the voltage window will decrease. (Actually, for other reasons, operation is limited to about 1900 µA.) Here, in addition, a 1 MΩ isolation resistor can be placed much closer to the septum in vacuum (Fig. 1 R5, Fig. 2 bottom right), thereby reducing the charge consumed by the breakdown. With this, the cathode voltage deficit after 1 ms would decrease to 1 kV. We assume that in vacuum a resistor of 100 mm length will hold the full voltage which is applied for ~40 µs, although commercially available items are specified for much lower voltages for long-term operation in air. However, this has to be proven experimentally. If needed, the resistor may be prolonged to 180 mm.

In 2001, a similar proposal intended to speed up the charge exchange from the long cable by a lower-ohm external isolation resistor, eventually augmented by switching an additional charge from a dedicated storage capacitor [12]. With doubts that the isolation resistor would be able to prevent the charge from the long cable to be consumed in the breakdown, coupled with small value attached to the envisaged benefit, it was not pursued.

BREAKDOWN MECHANISM

A common approach to describe a sparkover in vacuum is that it starts with a point on the cathode, where plasma is generated, and the plasma is expanding towards the anode with a velocity of about 20 km/s (see, e.g., [13, 14]). In [15] a formula is derived to describe the time dependent voltage at a spark gap, which discharges a capacitance parallel to it. The ratio of voltage U to start voltage U_0 is described as $u = U/U_0 = [1 + Bz/2]^{-2}$ with time dependence

$$z = \frac{\tau^2}{2} + 0.244\left\{\frac{(1-\tau)^2}{2} - 1.5 + 3\tau + 3\ln(1-\tau) + \frac{1}{1-\tau}\right\}$$

and $\tau = vt/d$ the time relative to the time the plasma needs to cross the gap width d at a plasma velocity v, $B = \frac{A\sqrt{U_0}d}{vC}$ with constant $A = 3{\cdot}10^{-5}\,\mathrm{A/V^{1.5}}$, and C the capacitance to be discharged. The formula is valid for times $\tau < 1$, i.e. until the plasma has bridged the gap, and not too large capacitances, so that $B > 1$. Despite the complexity of the analytical formula, the results must be considered as a crude estimate. De facto, the plasma has heavy fluctuations and limited reproducibility.

In case the plasma has bridged the gap, the current is limited only by external components (e.g., cable inductance), and the gap voltage is given by the vacuum arc burning voltage of around 50 V. For continuous plasma generation, a current flow of a few Amperes is needed, otherwise the plasma would dissipate to the walls, and after a few µs the gap would be isolating again [16]. Hence, with an isolation resistor of 350 kΩ, a feeding of the discharge by the charge from the long cable is not likely, even in the case of reflections at not well-terminated ends of the transmission lines formed by the setup.

We evaluate the formula for 410 pF, 70 pF and 40 pF, which are assumed as discharged capacitances behind the isolation resistor in the variants of the LTspice simulation listed in Fig. 1, using $v = 20$ km/s as the plasma velocity, $d = 17$ mm as the gap distance and a starting voltage of $U_0 = 134$ kV. The time until the plasma has crossed the gap ($\tau = 1$) is, in our case, $t = d/v = 17$ mm/20mm/µs = 850 ns. Using $B = \frac{3{\cdot}10^{-5}\mathrm{A/V^{1.5}}\ \sqrt{134000\mathrm{V}}\ \ 0.017\mathrm{m}}{20000\mathrm{m/s}\ \ C}$, we find that for $C = 410$ pF, $B = 22.8$, for $C = 70$ pF, $B = 133$, and for $C = 40$ pF, $B = 233$.

The corresponding voltage decay curves are depicted in Fig. 5, together with the current $I = C{\cdot}\mathrm{d}U/\mathrm{d}t$. In all cases the capacitance is discharged before the spark plasma bridges the gap. However, whereas for the 410 pF capacitance the decay to 10% of original voltage takes nearly 500 ns, it needs only 220 ns with 70 pF and only 160 ns with 40 pF. Currents are decayed to a few Amperes a little later, and hence we expect that the cathode is close to fully discharged when the gap gets isolated again. This corresponds well with the observed occurrence of a standard load curve.

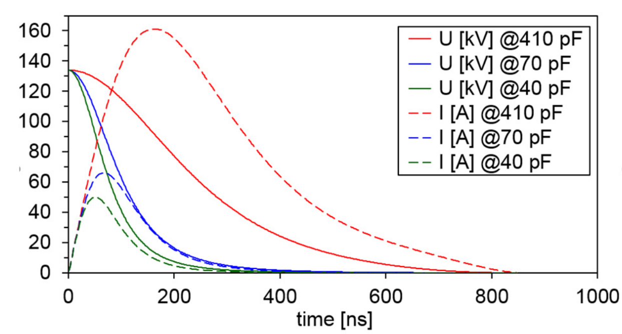

Figure 5: Voltage and current during sparkover.

OTHER ASPECTS

At the larger extraction septum EEC, capacitance and actual and improved recharge time are nearly doubled. However, the effect on damage caused by the beam will be counteracted by the initially lower stopping power and scattering of the lost higher energy protons. Also, for EEC, the total width of the usable septum voltage window already shrinks from 26 kV to 11 kV when the beam current is increased from 1330 µA to 1730 µA. This can be studied in detail, when the higher beam current is available again.

ISBN: 978-3-95450-205-9 doi:10.18429/JACoW-Cyclotrons2019-MOP025

At a breakdown, the beam interlocks triggered by loss-monitors and low-voltage indication must be suppressed for about a ms. But in case of a repeated breakdown, the beam should be switched off to prevent damage.

In case of a breakdown, the feedback control of the amplifiers of the acceleration cavities could cope with the sudden drop of beam current. However, the regulation of the actual flat-top cavity amplifier, which is already at its limits, would not [17]. An upgrade of the cavity, which is under discussion for other reasons, would be required.

CONCLUSION

Based on the developed understanding, we assume that the proposed changes would allow keeping the beam running over individual discharges of the injection and extraction septa of the Ring cyclotron.

AUTHOR CONTRIBUTIONS

RD initiated this work, performed the measurements and LTspice simulations and wrote the manuscript. JB contributed the breakdown theory and suggested the in-vacuum isolation resistor. Both discussed the whole topic and verified the paper.

ACKNOWLEDGEMENTS

We like to thank Martin Baumgartner, Dietmar Götz and Thomas Rauber for providing information on the built-in septa, cables, resistors and power supplies. We thank Dr. Bräunlich from FKH for useful comments and literature. Thanks to Steffen Schnabel for help with LTspice and to Oliver Dölling for cleaning the underlying drawings for Fig. 2.

REFERENCES

[1] M. Olivo, “The electrostatic extractor channel for the SIN 590-MeV ring cyclotron”, in *Proc. Cyclotrons'75*, Zurich, Switzerland, Aug. 1975, paper D-18, pp. 292-296.

[2] M. Seidel, J. Grillenberger, and A. C. Mezger, “High intensity operation and control of beam losses in a cyclotron based accelerator”, in *Proc. HB'12*, Beijing, China, Sep. 2012, paper THO1C01, pp. 555-559.

[3] S. Janssen, Paul Scherrer Institute, private communication, June 2019.

[4] B. Blau *et al.*, “Investigations on the premature failure of SINQ target #11 and its countermeasures”, to be presented at ICANS XXIII, Chattanooga, USA, Oct. 2019, to be published.

[5] D. Reggiani, “Extraction, transport and collimation of the PSI 1.3 MW proton beam”, in *Proc. HB'12*, Beijing, China, Sep. 2012, paper WEO3A03, pp. 373-377.

[6] R. Dölling, E. Johansen, M. Roggli, W. Koprek, and D. Llorente Sancho, “Development of new loss monitor electronics for the HIPA facility”, presented at the IBIC’19, Malmö, Sweden, Sep. 2019, paper MOPP024.

[7] D. Götz, PSI, private communication, May 2019.

[8] R. Dölling *et al.*, “Development of a replacement for the long radial probe in the ring cyclotron”, presented at Cyclotrons'19, Cape Town, South Africa, Sep. 2019, paper MOP024, this conference.

[9] `http://dielectricsciences.thomasnet.com/Asset/2134.pdf`

[10] `https://www.analog.com/en/design-center/design-tools-and-calculators/ltspice-simulator.html`

[11] J. Borburgh, CERN, private communication, May 2019.

[12] R. Dölling, “Möglichkeit einer schnellen Regeneration der Spannung elektrostatischer Elemente nach Durchschlägen”, Paul Scherrer Institute,, Villigen, Switzerland, Internal Rep. HIPA-ELSTAT-DR84-003.00-100801, Aug. 2001.

[13] B. Jüttner, “Vacuum breakdown”, *Nucl. Instrum. Methods Phys. Res.*, *Sect. A*, vol. 268, pp. 390-396, 1988.

[14] G. A. Mesyats and D. I. Proskurovski, “Pulsed electrical discharge in vacuum”, Springer Verlag, 1989.

[15] Jörg Brutscher, “Experimentelle und theoretische Untersuchungen zum Hochvakuumdurchschlag”, Ph.D. thesis, Frankfurt 1992.

[16] H. J. Lippmann, “Schalten im Vakuum”, VDE Verlag 2003.

[17] M. Schneider, Paul Scherrer Institute, private communication, July 2019.